



Specific absorption rate and temperature elevation in the human head due to overexposure to mobile phone radiation with different usage patterns



Deepshikha Bhargava^a, Nopbhorn Leeprechanon^a, Phadungsak Rattanadecho^{b,*}, Teerapot Wessapan^c

^a Department of Electrical and Computer Engineering, Faculty of Engineering, Thammasat University (Rangsit Campus), Pathumthani 12120, Thailand

^b Center of Excellence in Electromagnetic Energy Utilization in Engineering (CEEE), Department of Mechanical Engineering, Faculty of Engineering, Thammasat University (Rangsit Campus), Pathumthani 12120, Thailand

^c School of Aviation, Eastern Asia University, Pathumthani 12120, Thailand

ARTICLE INFO

Article history:

Received 3 May 2018

Received in revised form 5 November 2018

Accepted 5 November 2018

Keywords:

Electromagnetic radiation

Mobile phone

Specific absorption rate

Temperature distribution

Finite element method

ABSTRACT

Accidental overexposure to non-standard mobile phone radiation can occur in many situations. The over-power limit of mobile phone radiation interacts with the human body which could result in an adverse effect on human health. It is envisaged that the severity of the physiological effect can take place with small temperature increase in the delicate organs or tissues such as eyes, brain, skin, etc. However, the resulting thermo-physiological response of the body tissues to overpower limit of mobile phone radiation is still not well implemented. The aim of this study is to analyze the effect of overexposure of mobile phone radiation on the specific absorption rate (SAR) and temperature increase in three-dimensional heterogeneous human head models. The study focuses attention on the differences in the electromagnetic (EM) absorption characteristics with higher power level among different usage pattern. The effect of three different usage patterns - voice calling, video calling, and texting- on SAR and temperature distributions in different types of head tissues is systematically investigated. This paper also investigates the effects of different user ages, radiated powers, and gap distances between mobile phone and human heads, on SAR and temperature distributions. Results obtained from this analysis considering the safety guidelines show a high impact of mobile phone radiation in the voice calling position. Hence, comparisons of the absorption of mobile phone radiation are calculated between an adult and a 7-year-old child head model, for the voice calling position at different gap distances. In addition, the results indicate that child head always has a higher absorption rate of mobile phone radiation than the adult head. The rate of absorption in tissue increases as the distance between mobile phone and head decreases and the radiated power increases, depending on their dielectric and thermal properties. The obtained results can be helpful in determining exposure limits for the power output of the mobile phone, and the distance a user should maintain from the mobile phone in thermo-physiological aspects.

© 2018 Elsevier Ltd. All rights reserved.

1. Introduction

The rapidly increasing concern of mobile phone radiations affecting human health has adversely been gaining much attention over nearly two decades. Many organizations such as Institute of Electrical and Electronics Engineers (IEEE) and the International Commission of Non-Ionizing Radiation Protection (ICNIRP) have established guidelines and standards based on peak specific

absorption rates, to limit the exposure of the electromagnetic field [1–3]. When exposed to EM radiation, biological tissues absorb EM radiation energy. Later, this absorbed energy gets converted into heat which leads to an increase in temperature of the tissues. A very small temperature increase of up to 0.2–0.3 °C in the hypothalamus and 3–4 °C in eye is able to alter the thermoregulatory behavior [4], and formation of cataract [5], respectively. However, in a real situation, it is not possible to directly measure the temperature increase in the body. Therefore, to understand the actual process of interaction between EM radiation and human organs, modeling of heat transfer in human tissues is necessary [6–9].

The study of the coupled model of EM wave and bio-heat equation in the tissues has been carried out from decades [10–13].

* Corresponding author.

E-mail addresses: bhargavadeepshikha38@gmail.com (D. Bhargava), nopbhorn@engr.tu.ac.th (N. Leeprechanon), ratphadu@engr.tu.ac.th (P. Rattanadecho), teerapot@eau.ac.th (T. Wessapan).

Nomenclature

C	specific heat capacity (J/(kg K))
E	electric field intensity (V/m)
f	frequency of incident wave (Hz)
j	current density (A/m ²)
k	thermal conductivity (W/(m K))
r	normal vector
Q	heat source (W/m ³)
T	temperature (K)
t	time

Greek letters

μ	magnetic permeability (H/m)
ε	permittivity (F/m)

σ	electric conductivity (S/m)
ω	angular frequency (rad/s)
ρ	density (kg/m ³)
ω_b	blood perfusion rate (1/s)

Subscripts

b	blood
ex	external
me	metabolic
r	relative
0	free space, initial condition

Many investigations have shown the effect of mobile phone radiation on the human head. Nonetheless, a majority of them only investigate the maximum SAR values permitted by public safety standards and do not discuss the electric field and temperature distribution in the tissues [14–17]. This causes an incomplete analysis of the results.

Our previous work discussed the temperature increase in biological tissues and has shown the importance of considering it in the tissues along with the SAR when exposed to EM radiation [13,18–20]. Keangin et al. [13] performed numerical analysis of microwave ablation technique in a liver tissue using single and double slot coaxial antennas that calculated microwave power absorbed, SAR, and temperature distribution in the tissues. Wessapan et al. [18] used a coupled model of EM wave propagation and heat transfer to obtain the SAR and temperature increase in a 3-D realistic human head model exposed to mobile phone radiation. Wessapan et al. [19] investigated the effect of operating frequency on SAR and temperature increase, in a heterogeneous human eye model exposed to EM fields. Recently, Wessapan et al. [20] investigated the temperature increase in the reproductive system of the male due to near-field EMF absorption.

The EM absorption in near-field exposure depends on several things, such as operating frequency of the mobile phone, distance between the mobile phone and human head, etc. Moreover, the new generation smartphones are used in many more ways than just making voice calls, for instance in short messaging service (SMS), video applications, and so on. Using the mobile phone in these contexts require different positions which cause the human head as well as the eyes to get exposed to the mobile phone radiation from different angles. Above that, children's heads are smaller in size and shape than the adults. The tissues of a child's head are thinner. This gives us a reason to assume that the penetration and distribution of EM field in child head is likely to be more [16,21–24]. The exposure guidelines are established on the bases of a head, size of an adult's, regardless of the fact that user's head varies according to their age and other parameters [25]. Also, there are many mobile phone models that are being built poorly by using low-quality components and are available at a cheaper price in the market. The performance of these mobile phones is obviously low level in terms of communication. But, there continuous use can also contribute to affecting the human health adversely. Generally, a normal mobile phone radiates 1–2 W of power. However, the low quality mobile phones may radiate more power in some situations, which may cause the human head to get exposed to the overexposure radiation. This type of case can lead to a more adverse impact on the human head. Therefore, it is necessary to systematically study the effect of different usage patterns on SAR and temperature

increase in adult's and children's heads to adequately explain the biological effects of mobile phone radiation on human head in a more realistic situation.

The first part of this paper will analyze the effect of the various usage patterns of mobile phone on an adult head. The second part represents the comparison between the adult and child head models for voice calling position. The work discussed in this paper is the extended version of our previous work [18,26] by further focusing on the effect of the usage patterns in overexposure condition. The head models used in this study are consist of various layers of human tissues such as skin, fat, bone, brain, and eyes. Electromagnetic wave propagation and heat transfer in the human head are calculated by using Maxwell's equations [18], and Pennes' bio-heat equations [6], respectively. The effect of the overexposure condition of mobile phone on the SAR and temperature distributions within the human head, while using it in different contexts (voice calling, video calling and, texting positions) are systematically analyzed.

2. Problem formulation*2.1. Head and mobile phone models*

Exposing humans to the EM field is considered against ethics. Hence, developing a structure through numerical simulation that represents a human head model as truly as possible is more suitable. An adult head model and a 7-year-old child head model are used in this study. The models are comprised of five tissues: skin, fat, bone, brain, and eye, shown in Fig. 1 (a). The geometries of 3D human head models shown in Fig. 1(c) and Table 1, are directly taken from the statistical body size data [18]. A patch antenna is used in this study, shown in Fig. 1(b). The antenna used transmits the radiated power up to 5 W with the frequency of 900 MHz.

2.2. Elements of study

The aim of this study is to find out the effect of mobile phone over-exposure condition and its different usage patterns on the SAR and temperature increase in the head models of adult and child. Three cases of different usage patterns of mobile phone are used for the study (Fig. 2). In the first case, for the voice calling position, the patch antenna is placed at a distance of 0.5 cm from the head, shown in Fig. 2(a). In the second case i.e. video calling case, the mobile phone is kept at a distance of 3 cm from the eye (Fig. 2(b)). For the third case i.e. texting case, mobile phone is slightly tilted with respect to the head, and placed at 6 cm distance

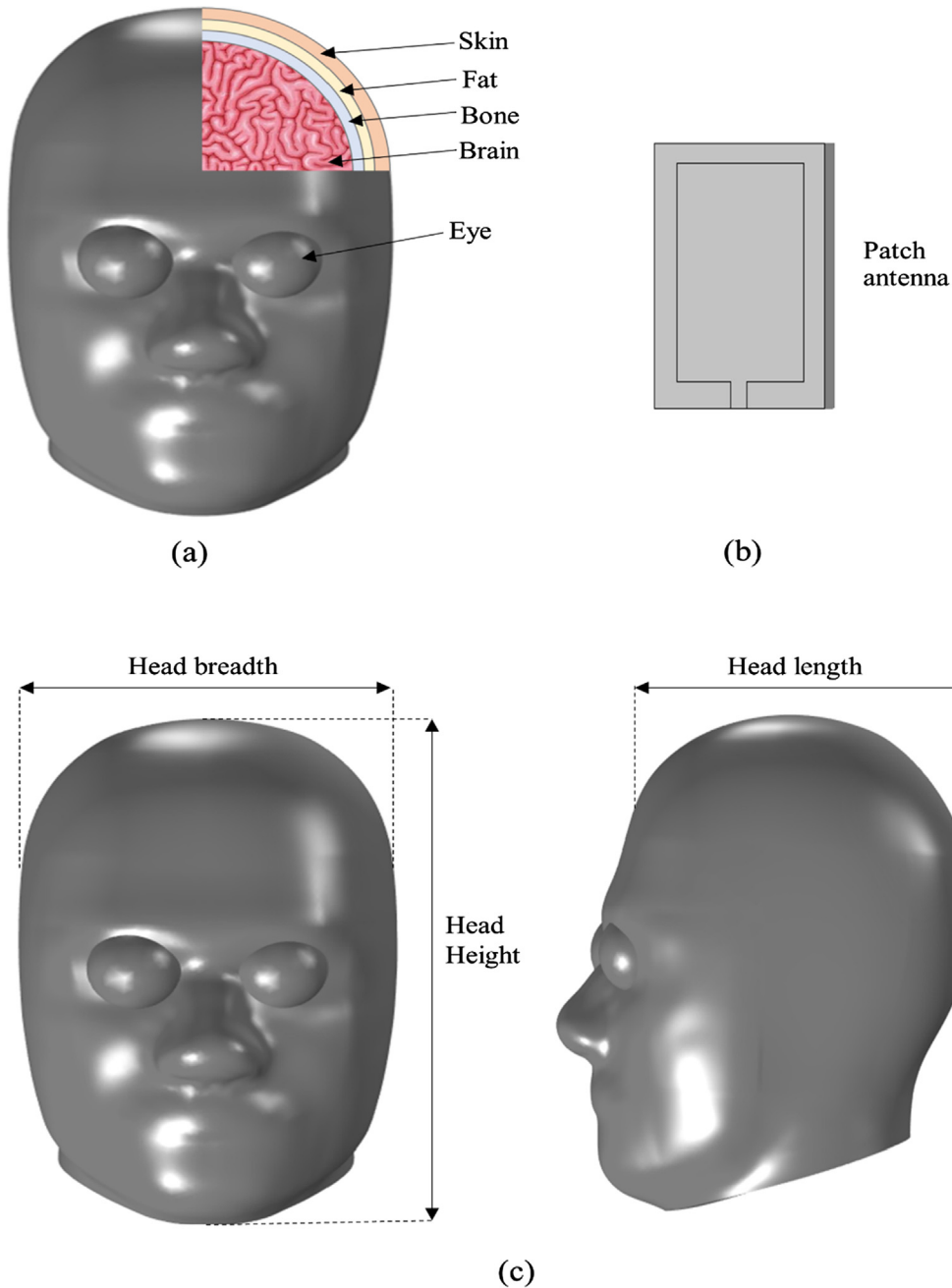


Fig. 1. The physical domains of the problem: (a) cross section of human head model, (b) patch antenna, and (c) dimensions of human head model.

Table 1
Head dimensions used in this study [18].

	Adult (cm)	7 years old child (cm)
Head length	28.99	17.3
Head breadth	24.69	14.9
Head height	36.03	20.8

(texting position) from the chin, shown in Fig. 2(c). The dielectric and thermal properties of the tissues used for the investigation are shown in Tables 2 and 3 [10,18,22]. In which ϵ_r and σ are the relative permittivity and electrical conductivity of the tissues, respectively. It is to be noted that there is no sufficient data for the thermal properties of the children; hence, it is assumed that there is no significant difference between the adult and children.

2.3. Equations for EM wave propagation analysis

To simplify the computational analysis, some of the following assumptions are made in the study:

1. The propagation of EM wave is modeled in three dimensions.
2. The EM wave interacts directly to the human head in the open region.
3. The free space outside the head model is truncated by using scattering boundary condition.
4. The dielectric properties of tissues are uniform and constant.

The EM wave propagation is solved by using Maxwell's equation which is simplified to demonstrate the EM field that penetrates into the human head [18,23], as follows;

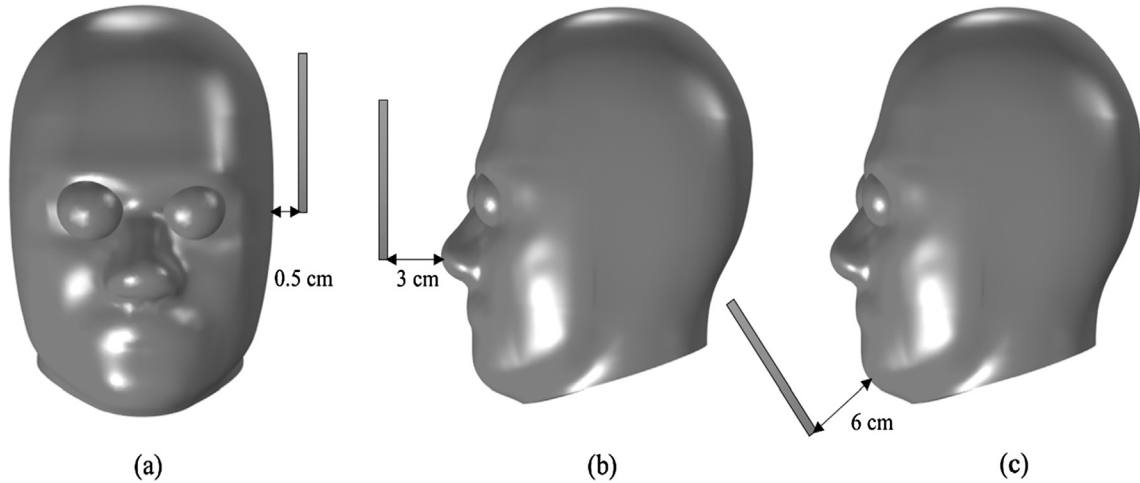


Fig. 2. Different positions of mobile phone model: (a) voice calling, (b) video calling, and (c) texting.

Table 2
Dielectric properties of tissues [14,18,22].

Types of tissues	Adult		7 years old	
	ϵ_r	σ (s/m)	ϵ_r	σ (s/m)
Skin	41.41	0.87	42.47	0.89
Fat	11.33	0.11	12.29	0.12
Bone	20.79	0.34	21.97	0.36
Brain	45.80	0.76	46.75	0.78
Eyes	36.59	0.51	49.60	0.99

$$\nabla \times \frac{1}{\mu_r} \nabla \times E - k_0^2 \epsilon_r E = 0 \quad (1)$$

where E is electric field intensity (V/m), μ_r is relative magnetic permeability, ϵ_r is relative dielectric constant, and k_0 is the free space wave number (m^{-1}).

2.3.1. Boundary condition for wave propagation analysis

In the patch antenna, a lumped port is defined at the bottom of the antenna and between the two patches of perfect electric conductor (Fig. 3). The lumped port is used for generating electromagnetic field by defining a voltage drop with specific radiated power, and can be written as follows:

$$Z_{in} = \frac{V_1}{I_1} = \frac{E_1 l_1}{I_1} \quad (2)$$

where Z_{in} is the input impedance (ohm), V_1 is the voltage along the edges (V). I_1 is the electric current magnitude (A), E_1 is the electric field along the source edge (V/m) and l_1 is the edge length. The perfect electric conductor boundary condition is applied along the patches of the antenna and is expressed as follows:

$$n \times E = 0 \quad (3)$$

Table 3
Thermal properties of tissues [10,18,19].

Tissue	ρ (kg/m ³)	k (W/m °C)	C (J/kg °C)	Q_{met} (W/m ³)	ω_b (1/s)
Skin	1125	0.42	3600	1620	0.02
Fat	916	0.25	3000	300	4.58×10^{-4}
Bone	1990	0.37	3100	610	4.63×10^{-4}
Brain	1038	0.53	3650	7100	8.83×10^{-3}
Eyes	1050	0.58	4178	0	0

In order to avoid reflections of emitted electromagnetic wave, a 3D spherical PML domain is created around the head models. Scattering boundary condition is applied on the outer surface of the PML domain, as expression:

$$n \times (\nabla \times E) - jkn \times (E \times n) = -n \times (E_0 \times jk(n - k)) \exp(-jk \cdot r) \quad (4)$$

where k is the wave number (m^{-1}), n is the normal vector, $j = \sqrt{-1}$, and E_0 is the incident plane wave (V/m).

2.4. Interaction of electromagnetic waves and human tissues

The EM wave propagating in 3-D, incident on the head model and the energy gets absorbed by the tissues. The absorbed EM energy is measured in term of SAR, which is defined as power dissipation rate normalized by material density [22,27]. The SAR is described by the following equation:

$$SAR = \frac{\sigma}{\rho} |E|^2 \quad (5)$$

where E is electric-field intensity (V/m), σ is electric conductivity (S/m), and ρ is the tissue density (kg/m³).

2.5. Equations for heat transfer analysis

For solving the thermal problem, the temperature distribution within the head models is obtained by solving bio-heat equations, which takes into consideration heat conduction, blood perfusion, and external heating. Heat transfer analysis is modeled in three dimensions. To simplify the problem, the following assumptions are made:

1. The human head tissues are biomaterial with uniform and constant thermal properties.

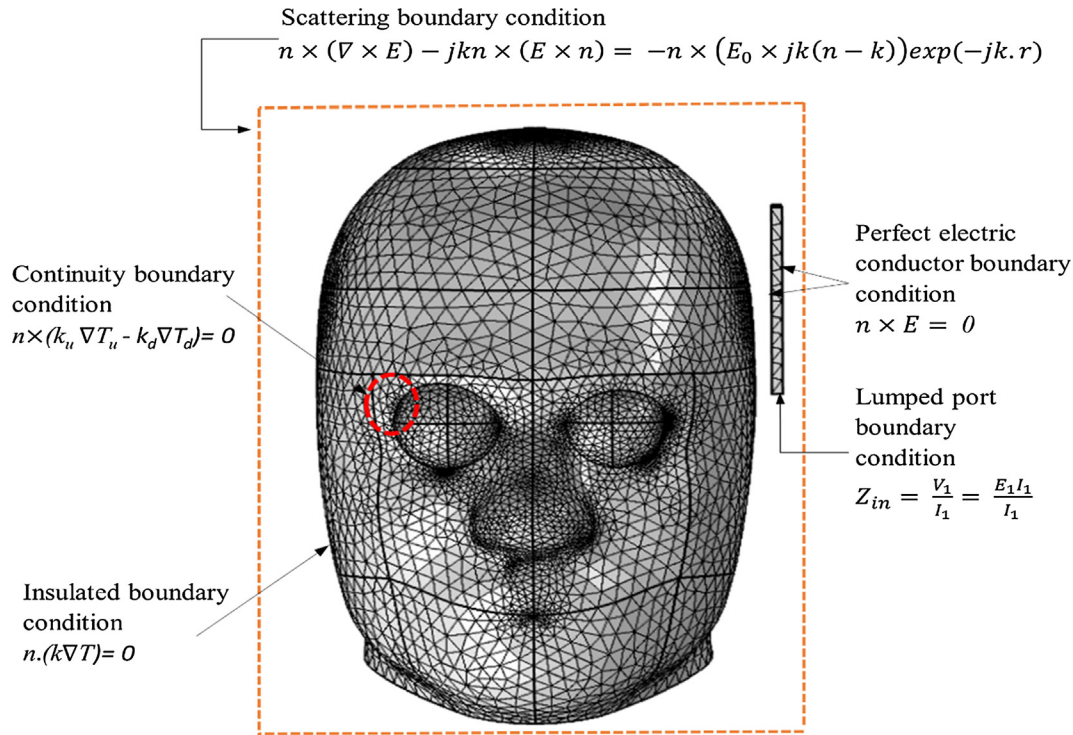


Fig. 3. Boundary conditions for analysis of electromagnetic wave propagation and heat transfer.

2. There is no phase change of substance within the tissue.
3. There is no energy exchange throughout the human head model.
4. There is no chemical reaction within the tissue.

Temperature distribution in the layers of human head are analyzed by solving Pennes' bio-heat equation [6,18]. The transient bio-heat equations, efficiently describe how the heat transfer occurs inside the human head, and can be written as:

$$\rho C \frac{\partial T}{\partial t} = \nabla \cdot (k \nabla T) + \rho_b C_b \omega_b (T_b - T) + Q_{met} + Q_{ext} \quad (6)$$

where ρ is the tissue density (kg/m^3), C is the heat capacity of tissue (J/kg K), k is thermal conductivity of tissue (W/m K), T is the tissue temperature ($^\circ\text{C}$), T_b is the temperature of blood ($^\circ\text{C}$), ρ_b is the density of blood (kg/m^3), C_b is the specific heat capacity of blood (J/kg K), ω_b is the blood perfusion rate ($1/\text{s}$), Q_{met} is the metabolism heat source (W/m^3) and Q_{ext} is the external heat source term (electromagnetic heat-source density) (W/m^3).

The heat conduction between tissue and blood flow is approximated by the blood perfusion term, $\rho_b C_b \omega_b (T_b - T)$. The external heat source term is equal to the resistive heat generated by electromagnetic field (electromagnetic power absorbed), which is defined as:

$$Q_{ext} = \frac{1}{2} \sigma_{tissue} |\bar{E}|^2 = \frac{\rho}{2} \cdot SAR \quad (7)$$

2.5.1. Boundary condition for heat transfer analysis

In this simulation, heat transfer is considered only in the human head, which does not include parts of the surrounding space. As shown in Fig. 3, the outer surface of the human head corresponding to assumption 3 is considered to be a thermally insulated boundary condition:

$$n \cdot (k \nabla T) = 0 \quad (8)$$

It is assumed that no contact resistance occurs between the internal organs of the human head. Therefore, the internal boundaries are assumed to be continuous:

$$n \cdot (k_u \nabla T_u - k_d \nabla T_d) = 0 \quad (9)$$

At the initial stage, the temperature distribution within the human head is assumed to be uniform at 37°C .

2.6. Numerical procedure

In order to develop an efficient numerical model of the human head exposure to mobile phone radiation, and determine the spatial distribution of the SAR and temperature within the model exposed to the mobile phone radiation, we utilized COMSOLTM Multiphysics which is based on finite element method (FEM) for solving all formulations. In FEM, the key step is to create the mesh of elements before performing any computation. Hence, different types of meshes such as triangular, swept, etc. are applied for spherical PML boundaries and the human head located within it, as shown in Fig. 3. The model of bio-heat equations and Maxwell's equations are then numerically solved. Convergence test of the case of voice calling application is carried out at 900 MHz frequency to identify the independence of the appropriate number of required mesh elements. The convergence test leads to a grid with approximately 450,000 elements, it can be assumed that with this number of elements the accuracy of the numerical results is independent of the number of mesh elements. The convergence curve resulting from the convergence test is shown in Fig. 4.

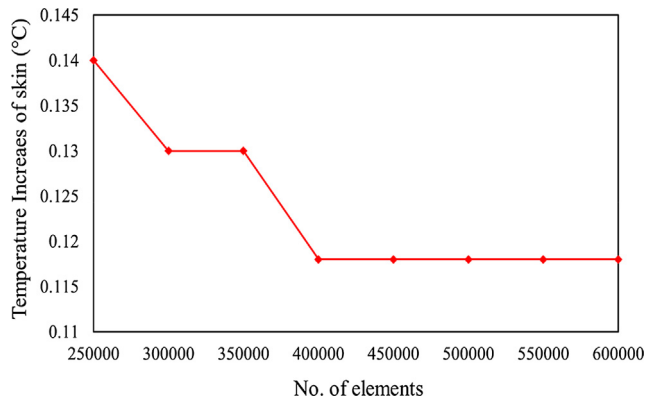


Fig. 4. The convergence curve of the 3D model.

3. Results and discussions

3.1. Numerical validation

To evaluate the accuracy of the current numerical model, we validate our results with the previously published paper of Wessapan et al. [18]. For this, the current numerical model has been modified and compared with the published work. The head model used for validation contains three layers – skin, fat, and bone. The patch antenna, operating at 900 MHz frequency and 1 W radiating power, is kept at the distance of 1 cm from the head model. The resulting SAR values from the present numerical model show fairly high agreement with the published work, as shown in Fig. 5. This favorable comparison lends confidence in the way of simulating the results of the present numerical model.

3.2. Calculation for adult head

3.2.1. Electric field distribution

To understand the electric field distribution inside each tissue of the human head, numerical analysis is required. Fig. 6 shows the comparison of the maximum electric field intensities inside each tissue layer of the human head exposed to the mobile phone radiation at 900 MHz frequency in voice calling, video calling, and texting positions, respectively. The analysis is performed for 60 min of mobile phone exposure, at the radiating power of 5 W. As shown in the figure, the highest and lowest electric field intensities among all the cases are found in the skin and brain layers of the human head, respectively. The maximum values of electric field intensities obtained in the head skin are 167.50 V/m, 99.17 V/m, and 36.06 V/m, in the voice calling, video calling, and texting positions, respectively. Whereas, for the eye, it is 24.45 V/m and 12.73 V/m, in the video calling and texting

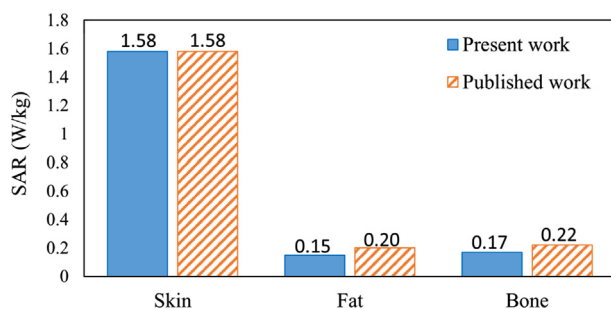


Fig. 5. Comparison of the calculated SAR distribution to the SAR distribution obtained by Wessapan et al. [18].

positions, respectively. A small distance between the mobile phone and the exposed model cause more electromagnetic absorption. Due to this, among all the cases, a greater value of electromagnetic distribution is found in the skin layer in the voice calling position (0.5 cm). Moreover, it is noted that electric field deep inside the head diminishes, because, the absorption of EM energy causes electric fields to attenuate, which later gets converted into heat. The dielectric properties shown in Table 2 play an important role in the absorption of EM energy. A higher value of electric field intensity obtained in the skin layer generates a high value of SAR. This explains the reason behind obtaining the highest value of SAR and electric field distributions in the skin layer for voice calling position.

3.2.2. SAR distribution

Fig. 7 shows the SAR distribution in the adult head model, for all the three cases (Fig. 2). The red area on the head models indicates the highly affected region due to the mobile phone exposure. The maximum SAR value of 10.84 W/kg for the voice calling position is obtained right beneath the antenna (Fig. 7(a)), which is the highest SAR in head skin among all the cases. In the video calling position (Fig. 7(b)), the maximum SAR value for the skin region is found on the tip of the nose, right in front of the mobile phone with the value of 3.80 W/kg. Whereas, in the texting position (Fig. 7(c)), the maximum SAR value for skin is shown on the upper lip area of the human head with the value of 0.51 W/kg. Fig. 8 shows the bar graph representation of the comparison of maximum SAR values for all three cases. It was found that the highest value of SAR, which corresponds to Eq. (5), always obtained in the skin layer for every case. The maximum SAR values in the tissues are found to be correlated with the electric field intensities (Fig. 6). It can be seen that the SAR values in each tissue layer decrease rapidly along the distance from the mobile phone. It is evident that the magnitude of dielectric properties in each tissue, shown in Table 2, highly influence the SAR distribution within the human head. For the eyes, values of maximum SAR distributions are 0.526 W/kg and 0.126 W/kg, in the video calling, and texting positions, respectively. The obtained values of maximum SAR in the skin layer in voice and video calling positions, with overexposure condition of 5 W radiated power, exceed the ICNIRP maximum exposure limit of 2 W/kg.

3.2.3. Temperature distribution

To illustrate the process of heat transfer in the human head, the coupled model of electromagnetic wave propagation and heat transfer is investigated numerically. Due to these coupled effects, the electromagnetic energy (Fig. 6) is absorbed by the tissue (Fig. 7) and later transformed into an incremental amount of heat. Fig. 9 shows temperature increase distribution in the adult head exposed to the mobile phone radiation in three cases. In the head skin, around the ear, the temperature increase is 0.19 °C (Fig. 9(a)), right beneath the region of the antenna in the voice calling case, which is the highest temperature in head skin among all the cases. In the video calling position (Fig. 9 (b)), the maximum temperature increase for the skin region is found on the tip of the nose, right in front of the antenna (0.05 °C). Whereas, in the texting position (Fig. 9(c)), the maximum temperature increase for skin is shown on the upper lip area of the human head (0.015 °C). Figs. 10 and 11 show the slice plot representation and the bar graph representation of the comparison of the maximum temperature distribution in the head layers for all the three cases, respectively. The slice plots shown in Fig. 10, depict the sensitive areas of the human head with an increased value of temperature in it. From Fig. 11, it is found that the maximum temperature increase does not directly correspond to the maximum SAR value (Fig. 8). As can be seen, the temperature in the fat layer is higher than the bone, even when the high value of SAR is found

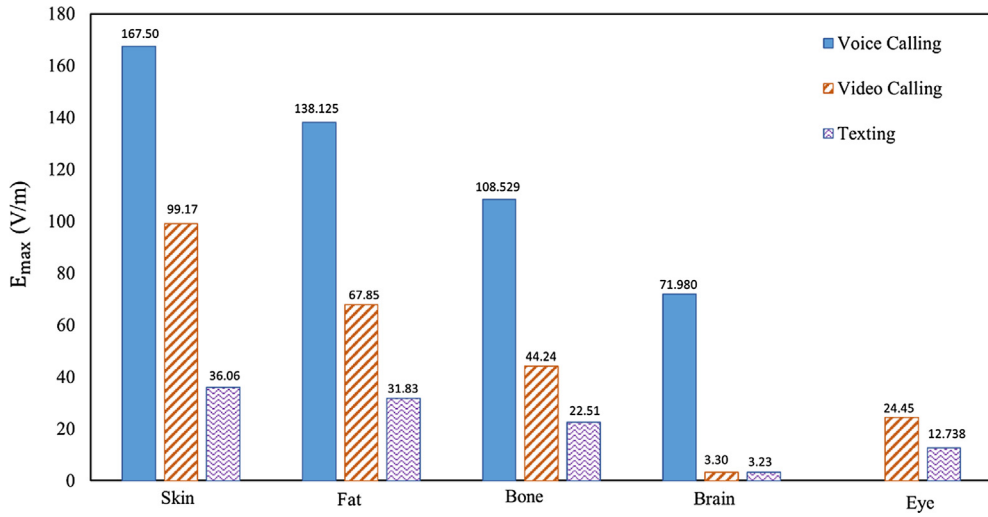


Fig. 6. Comparison of maximum electric field intensities (V/m) in adult head exposed to the 5 W radiating power, at the frequency of 900 MHz, for the time period of 60 min in, voice calling, video calling, and texting positions.

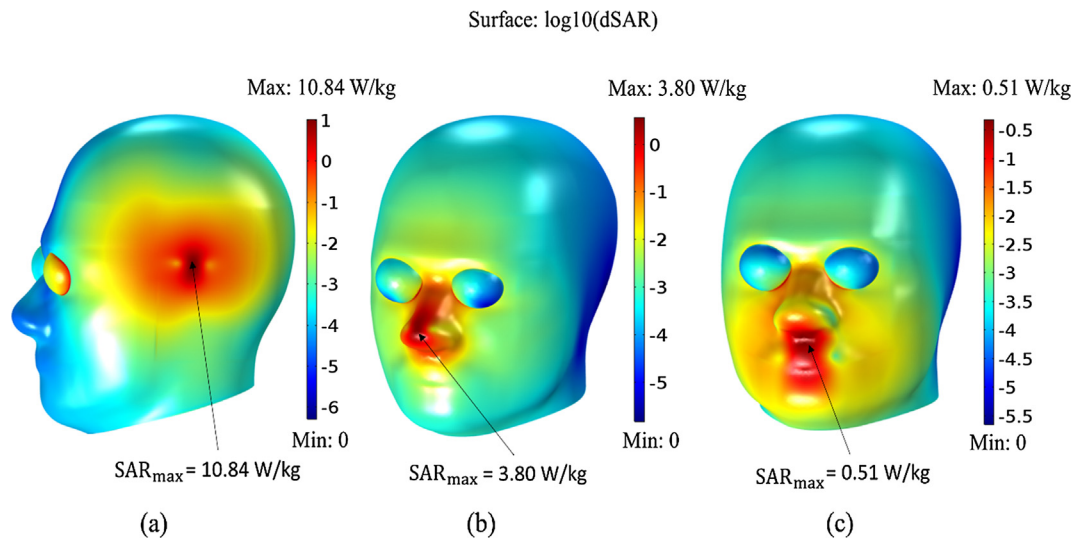


Fig. 7. SAR distribution in the adult head model exposed to the 5 W radiating power, at the frequency of 900 MHz, for the time period of 60 min in: (a) voice calling, (b) video calling, and (c) texting positions.

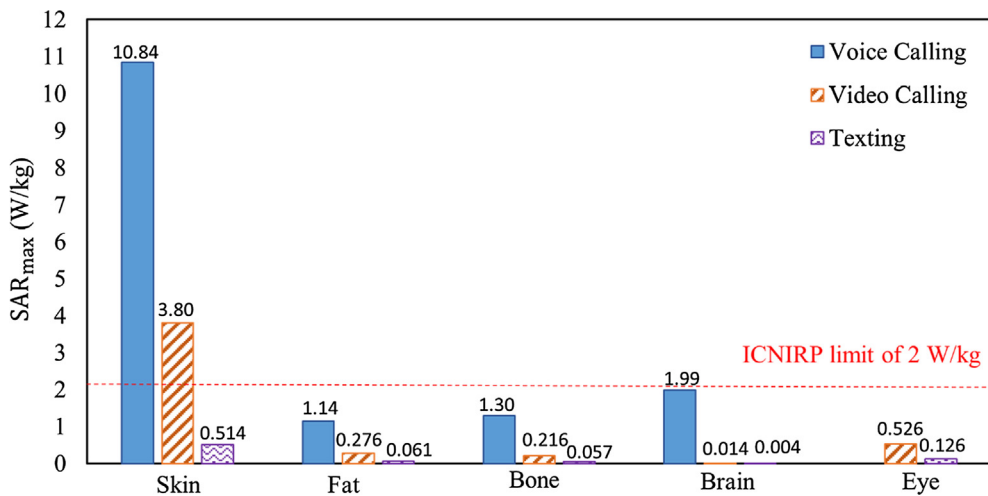


Fig. 8. Comparison of maximum SAR values (W/kg) in adult head exposed to the 5 W radiating power, at the frequency of 900 MHz, for the time period of 60 min in, voice calling, video calling, and texting positions.

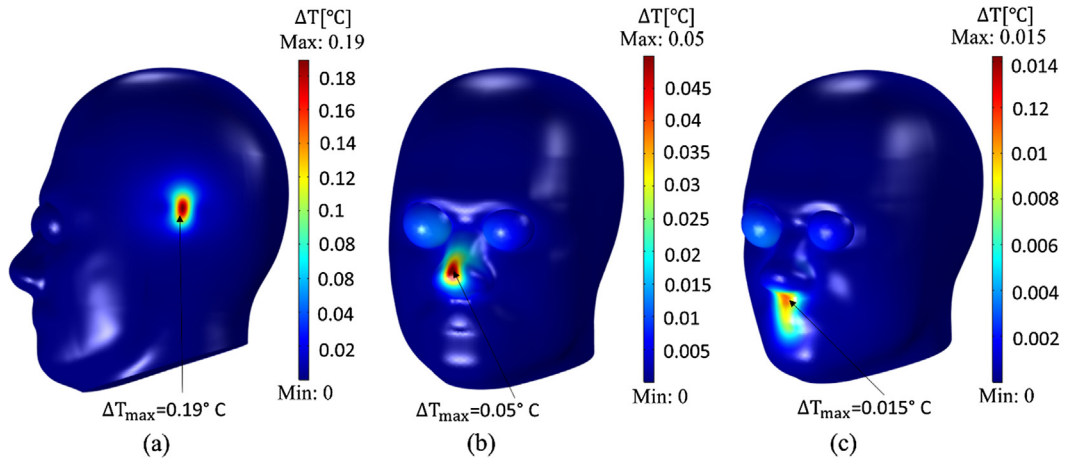


Fig. 9. Temperature increase distribution in the adult head model exposed to the 5 W radiating power, at the frequency of 900 MHz, for the time period of 60 min in, (a) voice calling, (b) video calling, and (c) texting positions.

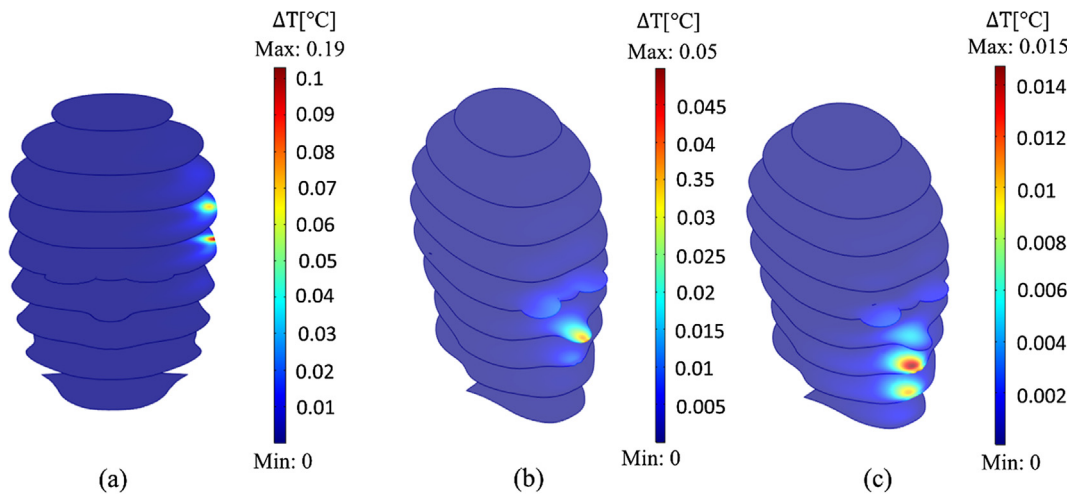


Fig. 10. Slice plot of temperature increase in the adult head model exposed to the 5 W radiating power, at the frequency of 900 MHz, for the time period of 60 min in, (a) voice calling, (b) video calling, and (c) texting positions.

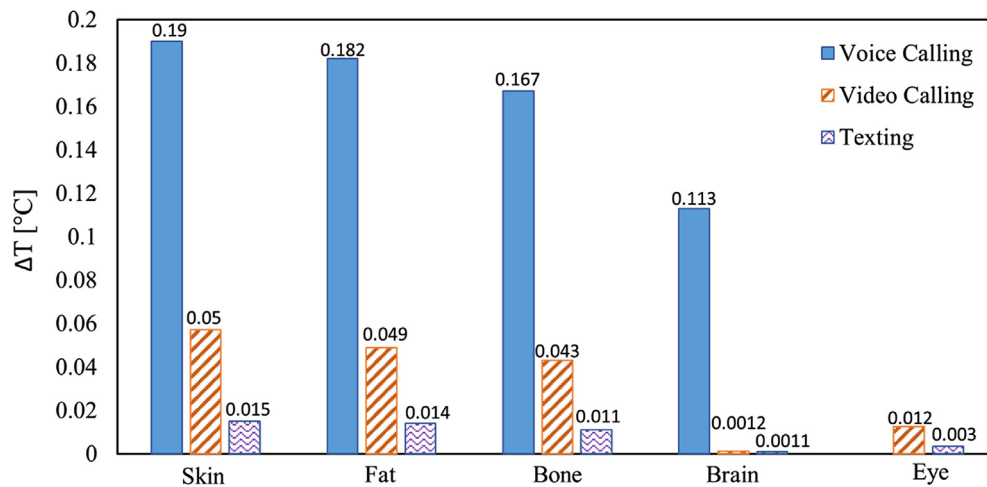


Fig. 11. Comparison of maximum temperature increases (°C) in adult head exposed to the 5 W radiating power, at the frequency of 900 MHz, for the time period of 60 min in, voice calling, video calling, and texting positions.

in bone compared to the fat for the voice calling case. This is because the lower value of blood perfusion rate in the fat layer keeps the temperature higher than the bone layer. Whereas the higher value of dielectric properties in the bone layer keeps the SAR higher than the fat layer. Also, due to the low value of thermal conduction of the fat, the temperature is higher there compared to the bone layer. The obtained temperature increase values are well below to cause any thermal damage [19]. It is noticed that the thermal properties of the tissue, shown in Table 3, highly influenced the temperature distribution. We need to raise awareness because an increase of approximately 0.2–0.3 °C temperature in the hypothalamus leads to altered thermoregulatory behavior [4], however, the obtained results are still well below the limited values.

3.3. Effect of gap distances on the adult and child head

In all of the above cases, the analysis was performed for the adult head and the highest values of SAR and temperature increase among all the cases were found for the voice calling position. Therefore, comparison of the distribution parameters has been made between the child and adult head models for the voice

calling case only. Fig. 12 shows the SAR and temperature increase in the child head model when the mobile phone is placed at a distance of 0.5 cm, at the frequency of 900 MHz, at the radiating power of 5 W, for the exposure time of 60 min. The SAR distribution shown in Fig. 12(a) is transformed into an incremental amount of temperature through EM absorption by the tissue in Fig. 12(b). Figs. 13 and 14 show the comparison of maximum values of SAR and temperature increase in the child and adult heads when the distance between the mobile phone and head varies from 0.5 cm to 1 cm, respectively. It is obvious from the figures that the value of SAR and temperature decrease as the mobile phone goes far away. Increasing the distance from 0.5 to 1 cm in the child head, causes the SAR to decrease by almost 61%. The temperature, however, decreases slowly compared to the SAR. It decreases to 58% by increasing the distance between mobile phone and head model to 1 cm. One can see the value of SAR and temperature distribution in child head are higher than the adult head. This is because the dielectric properties of child head are higher than the adult head which becomes the reason of higher absorption of EM energy. Also, the smaller size of the child head causes a deeper level of penetration of EM fields into the tissues. This all leads to higher value of SAR and temperature distribution in the child head.

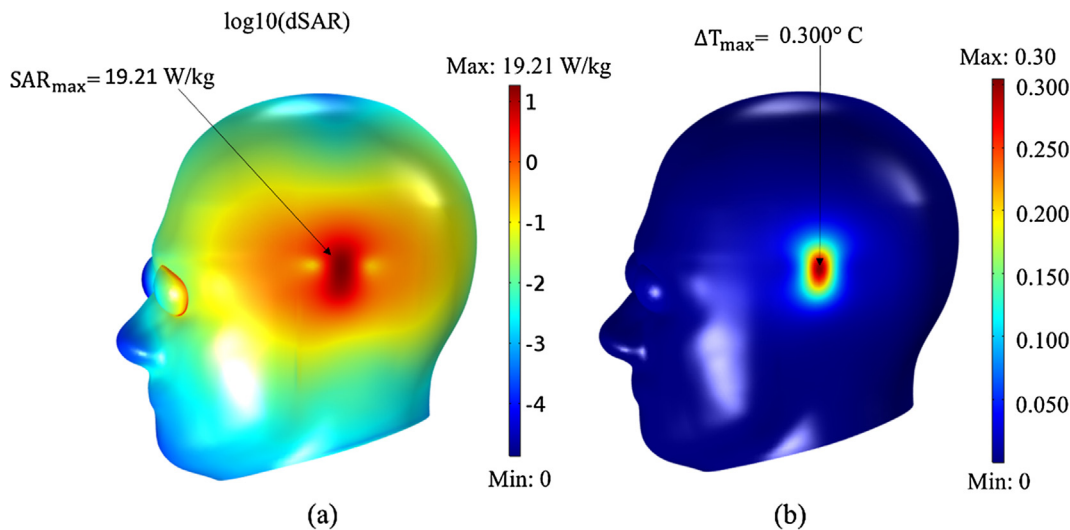


Fig. 12. Child head model exposed to mobile phone radiation working at 900 MHz frequency, at the radiating power of 5 W, for the time period of 60 min, for the gap distance of 0.5 cm. (a) SAR distribution (W/kg). (b) Temperature distribution (°C).

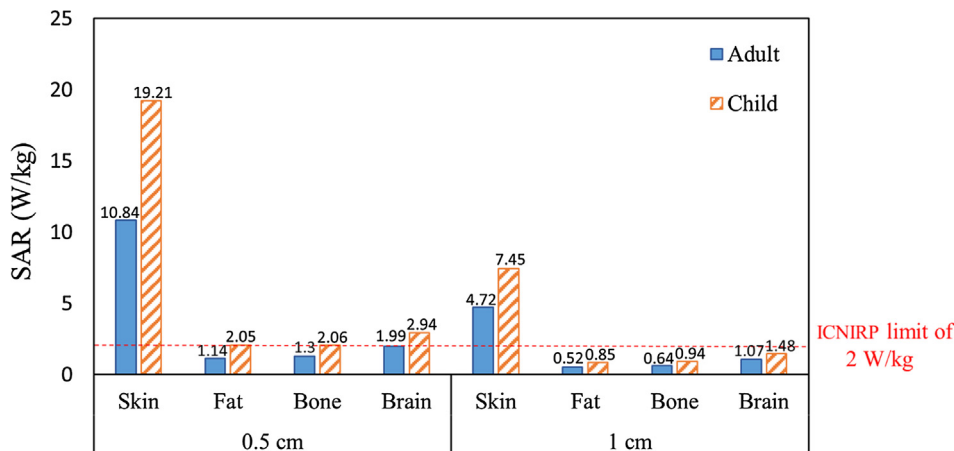


Fig. 13. Comparison of maximum SAR values (W/kg) in adult and child heads exposed to the 5 W radiated power, at the frequency of 900 MHz, at different gap distances, for the time period of 60 min in voice calling position.

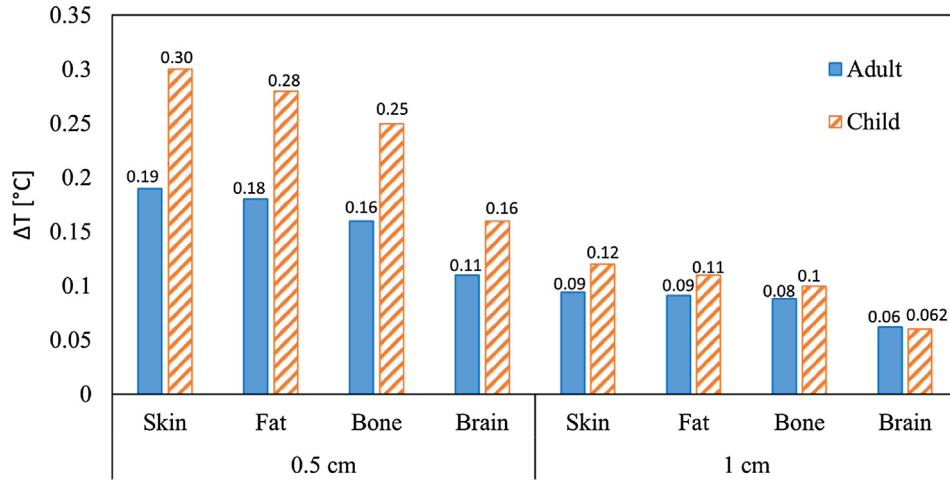


Fig. 14. Comparison of maximum temperature increases (°C) in adult and child heads exposed to the 5 W radiating power, at the frequency of 900 MHz, at different gap distances, for the time period of 60 min in voice calling.

By comparing to the ICNIRP exposure limit, the maximum value of SAR in child head for the 0.5 cm gap distance exceeds the limited value in every tissue. Whereas, for the 1 cm gap distance the SAR value in child head only exceeds in the skin layer. For adult, the SAR value exceeds the limited value only in the skin for both gap distances. Comparing to the temperature increase level for the hypothalamic region that may affect thermoregulatory response (0.2–0.3 °C) [4], the resulting value of maximum temperature increase in the brain region does not exceed this value in both gap distances.

3.4. Effect of different radiated powers on the adult and child head

The effect of the different radiated powers on the adult and child heads has also investigated. Recall from the previous section, skin layer of the human head has maximum values of SAR and temperature increase. Figs. 15 and 16 show the maximum value of SAR and temperature increase, respectively, in the skin layer, for the gap distance of 0.5 cm and various radiated power levels. It can be clearly seen from the graphs that the radiated power of mobile phone influences the distribution parameters. It is found that SAR and temperature increase within the head increase with the increase in radiated powers. The slopes correlating the maximum SAR in the head and the radiated powers are significantly affected by user age. From the analysis, the child head is found

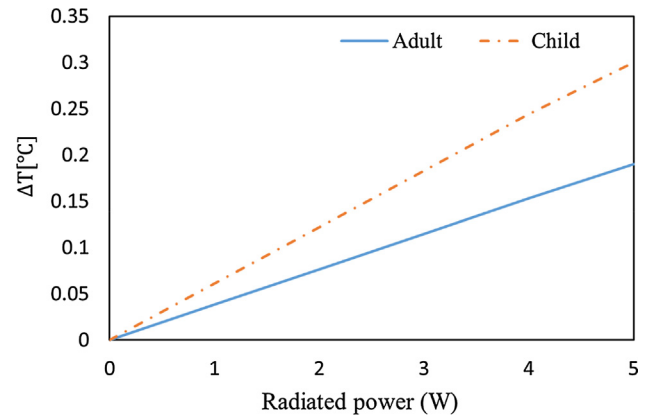


Fig. 16. Comparison of maximum temperature increases (°C) at different radiated powers in adult and child heads in voice calling position.

to be more sensitive than the adult head in both terms of SAR and temperature increase. The obtained SAR values from the radiated powers higher than 0.5 W and 0.8 W, in child and adult, respectively, are found to exceed the ICNIRP exposure limit [1]. However, the maximum temperature increase in the head tissues for all radiating powers does not lead to any physiological damage

4. Conclusion

The paper investigates the increase in SAR and temperature in anatomical human head models of child and adult in overexposure situations. The comparison of the three different mobile phone usage patterns is studied when the head models are exposed to mobile phone radiation at 900 MHz frequency and 5 W radiating power. The study also includes a comparison of the distribution parameters in child and adult heads, effect of different gap distances and radiated powers. The results show that among all the cases, the SAR and temperature increase are found to be highest in the voice calling case for 0.5 cm gap distance and 5 W radiated power. Also, it is evident from the results that the SAR and temperature increase in the tissues do not directly correspond to each other but are related to the physical parameters of biological tissues such as thermal conductivity, dielectric properties, blood perfusion rate, etc. This shows the importance of performing transient thermal analysis along with the dosimetry analysis to clearly understand the interaction between mobile phone radiation and

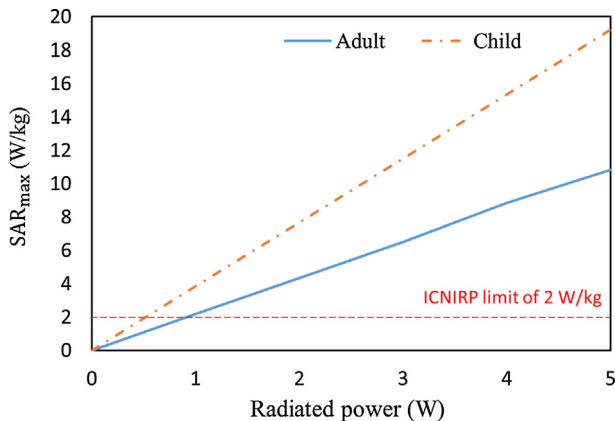


Fig. 15. Comparison of maximum SAR values in adult and child heads at different radiated powers in voice calling position.

human tissues. Comparing to the ICNIRP exposure limit, the resulting SAR values in skin layer, in voice and video calling cases, are found to exceed the exposure limit. But, comparing the temperature increase in the brain, it does not approach the possible physiological damage.

This study shows the concern regarding the non-standard mobile phone devices which may be harmful to human health from excessive radiation power. Moreover, the obtained results from the study also show that the children are more exposed and have a greater possibility of a serious adverse effect than the adult when exposed to mobile phone radiation.

5. Conflict of interest

The authors declare that there are no known conflicts of interest.

Acknowledgments

The Thailand Research Fund (Contract No. RTA 5980009) and The Thailand Government Budget Grant provided financial support for this study.

Appendix A. Supplementary material

Supplementary data associated with this article can be found, in the online version, at <https://doi.org/10.1016/j.ijheatmasstransfer.2018.11.031>.

References

- [1] ICNIRP Guidelines, Guidelines for limiting exposure to time-varying electric, magnetic, and electromagnetic fields (up to 300 GHz), *Health Phys.* 74 (1998) 494–522.
- [2] IEEE Standard for Safety Levels with Respect to Human Exposure to Radio Frequency Electromagnetic Fields, 3 kHz to 300 GHz, IEEE Std C95.1-2005 (Revision of IEEE Std C95.1-1991) (2006) 1–238.
- [3] D. Bhargava, N. Leeprechanon, A review of the effect of non-ionizing microwave radiation on human health science & technology asia, 22, 2017, 65–82.
- [4] A. Hirata, M. Morita, T. Shiozawa, Temperature increase in the human head due to a dipole antenna at microwave frequencies, *IEEE Trans. Electromagn. Compat.* 45 (2003) 109–116.
- [5] C. Buccella, V.D. Santis, M. Feliziani, Prediction of temperature increase in human eyes due to RF sources, *IEEE Trans. Electromagn. Compat.* 49 (2007) 825–833.
- [6] H.H. Pennes, Analysis of tissue and arterial blood temperatures in the resting human forearm, *J. Appl. Physiol.* 85 (1998) 5–34.
- [7] H. Arkin, L.X. Xu, K.R. Holmes, Recent developments in modeling heat transfer in blood perfused tissues, *IEEE Trans. Biomed. Eng.* 41 (1994) 97–107.
- [8] T.-C. Shih, H.-L. Liu, A.T.-L. Horng, Cooling effect of thermally significant blood vessels in perfused tumor tissue during thermal therapy, *Int. Commun. Heat Mass Transf.* 33 (2006) 135–141.
- [9] A. Joukar, E. Nammakie, H. Niroomand-Oscuii, A comparative study of thermal effects of 3 types of laser in eye: 3D simulation with bioheat equation, *J. Therm. Biol.* 49–50 (2015) 74–81.
- [10] A. Hirata, M. Fujimoto, T. Asano, W. Jianqing, O. Fujiwara, T. Shiozawa, Correlation between maximum temperature increase and peak SAR with different average schemes and masses, *IEEE Trans. Electromagn. Compat.* 48 (2006) 569–578.
- [11] A. Razmadze, L. Shoshiashvili, D. Kakulia, R. Zaridze, Correlation Between SAR and Temperature Rise Distributions with Different Masses and Schemes of Averaging, Child Head, Dipole Antenna Radiation at 1800 MHz, in: 2007 XIIth International Seminar/Workshop on Direct and Inverse Problems of Electromagnetic and Acoustic Wave Theory (2007) pp. 48–53.
- [12] A. Hirata, W. Jianqing, O. Fujiwara, M. Fujimoto, T. Shiozawa, Maximum temperature increases in the head and brain for SAR averaging schemes prescribed in safety guidelines, *Int. Symp. Electromagn. Compat.* 3 (2005) 801–804.
- [13] P. Keangin, P. Rattanadecho, T. Wessapan, An analysis of heat transfer in liver tissue during microwave ablation using single and double slot antenna, *Int. Commun. Heat Mass Transf.* 38 (2011) 757–766.
- [14] O.P. Gandhi, G. Lazzi, C.M. Furse, Electromagnetic absorption in the human head and neck for mobile telephones at 835 and 1900 MHz, *IEEE Trans. Microwave Theory Tech* 44 (1996) 1884–1897.
- [15] M.I. Hossain, M.R.I. Faruque, M.T. Islam, Analysis on the effect of the distances and inclination angles between human head and mobile phone on SAR, *Progr. Biophys. Mol. Biol.* 119 (2015) 103–110.
- [16] A. Hadjem, E. Conil, A. Gati, M.-F. Wong, J. Wiart, Analysis of power absorbed by children's head as a result of new usages of mobile phone, *IEEE Trans. Electromagn. Compat.* 52 (2010) 812–819.
- [17] K. Masumnia-Bisheh, M. Ghaffari-Miab, B. Zakeri, Evaluation of different approximations for correlation coefficients in stochastic FDTD to estimate SAR variance in a human head model, *IEEE Trans. Electromagn. Compat.* 59 (2017) 509–517.
- [18] T. Wessapan, P. Rattanadecho, Numerical analysis of specific absorption rate and heat transfer in human head subjected to mobile phone radiation: Effects of user age and radiated power, *J. Heat Transf.* 134 (2012) 121101.
- [19] T. Wessapan, P. Rattanadecho, Specific absorption rate and temperature increase in the human eye due to electromagnetic fields exposure at different frequencies, *Int. J. Heat Mass Transf.* 64 (2013) 426–435.
- [20] T. Wessapan, P. Rattanadecho, Temperature induced in the testicular and related tissues due to electromagnetic fields exposure at 900 MHz and 1800 MHz, *Int. J. Heat Mass Transf.* 102 (2016) 1130–1140.
- [21] A.A. de Salles, G. Bulla, C.E.F. Rodriguez, Electromagnetic absorption in the head of adults and children due to mobile phone operation close to the head, *Electromagn. Biol. Med.* 25 (2006) 349–360.
- [22] V. Stanković, D. Jovanović, D. Krstić, V. Marković, N. Cvetković, Temperature distribution and Specific Absorption Rate inside a child's head, *Int. J. Heat Mass Transf.* 104 (2017) 559–565.
- [23] B. Deepika, V. Ramya, T. Yamuna, R. Kalpana, A numerical analysis of temperature distribution in human eye when exposed to electromagnetic radiation, in: 2015 IEEE International Conference on Electronics, Computing and Communication Technologies (CONECCT), 2015, pp. 1–5.
- [24] A.I. Sabbah, Evaluation of SAR and temperature elevation in a multi-layered human head model exposed to RF radiation, Faculty of Graduate Studies Jordan University of Science and Technology M.Sc, *Electr. Eng.* (2010).
- [25] O.P. Gandhi, L.L. Morgan, A.A. de Salles, Y.-Y. Han, R.B. Herberman, D.L. Davis, Exposure limits: the underestimation of absorbed cell phone radiation, especially in children, *Electromagn. Biol. Med.* 31 (2012) 34–51.
- [26] T. Wessapan, S. Srisawatdhisukul, P. Rattanadecho, Specific absorption rate and temperature distributions in human head subjected to mobile phone radiation at different frequencies, *Int. J. Heat Mass Transf.* 55 (2011) 347–359.
- [27] A.I. Sabbah, N.I. Dib, M.d.A. Al-Nimr, SAR and temperature elevation in a multi-layered human head model due to an obliquely incident plane wave, *Progr. Electromagn. Res.* 13 (2010) 95–108.